



Universidad
del País Vasco

Euskal Herriko
Unibertsitatea



Master Interuniversitario en Nuevos Materiales

TRABAJO FINAL DE MASTER

Modificación de nanotubos de carbono mediante tratamientos químicos (Modification of carbon nanotubes by chemical treatments)

Presentado por: Javier Otero Márquez

**Realizado en: Departamento de Química e
Ingeniería de Procesos y Recursos.
Universidad de Cantabria.**

**Bajo la dirección de: M. Carmen Pesquera
González**

Santander, 3 de Julio de 2015

Resumen

Los nanotubos de carbono se consideran como uno de los posibles materiales que pueden conseguir importantes logros en el campo de la nanobiotecnología. Sin embargo, en el caso de los nanotubos de carbono multipared, sus superficies son hidrofóbicas e inertes, lo que provoca que sea complicado emplearlos. A través de tratamientos ácidos que originan su oxidación, es posible funcionalizarlos y mejorar su comportamiento hidrofílico, haciéndoles más solubles y reduciendo su toxicidad.

Esto se ha llevado a cabo mediante un tratamiento ácido con una mezcla de H_2SO_4/HNO_3 para diferentes tiempos. Con estos tratamientos, es importante establecer una relación entre los parámetros de la oxidación (concentración de los ácidos, tiempo de tratamiento y la temperatura) y el deterioro que el nanotubo es capaz de aguantar sin mermar sus propiedades mecánicas y electrónicas.

Los grupos funcionales introducidos mediante esta oxidación han reducido las interacciones de Van der Waals entre las paredes, mejorando la solubilidad. Además, se ha reducido la cantidad de impurezas, disminuyendo la toxicidad.

Las propiedades estructurales y de textura de los nanotubos tratados han sido analizados mediante distintas técnicas. Los principales cambios observados mediante espectros IR y análisis térmicos han sido un incremento en los grupos carboxilos, y en la temperatura de oxidación al aumentar el tiempo de tratamiento. Mediante espectroscopía Raman se ha estimado el desorden presente, el cual decrece para tiempos de oxidación cortos, para posteriormente aumentar a mayor tiempo.

Respecto a las propiedades de texturales obtenidas mediante isothermas de adsorción-desorción de nitrógeno, nos han permitido determinar la superficie específica, la cual aumenta con el tiempo de oxidación, y la distribución de tamaño de poro.

Palabras clave: MWCNT, nanotubos funcionalizados, tratamiento ácido, oxidación leve

Abstract

Carbon nanotubes (CNTs) are an important group of nanomaterials that have been proposed for the potential advancement of nano-bio-technology. However, the surfaces of multiwalled carbon nanotubes (MWCNTs) are hydrophobic and inert, which make them extremely difficult to work with in many applications. Surface functionalization by oxidizing the nanotubes using acid treatments is an attractive method for improving the hydrophilic behavior. These treatments make MWCNTs more soluble and reduce their toxicity.

In this work, we have attempted to improve the MWCNT's properties via oxidation treatments with a mild mixture of $\text{H}_2\text{SO}_4/\text{HNO}_3$ for different times. When applying these treatments, it is important to establish a relationship between the functionalization parameters (acid concentration, treatment time and temperature) and the damage the nanotube can support without deteriorating its mechanical and electronic properties.

The functional groups introduced by this treatment leads to a reduction of the Van der Waals interactions which improves MWCNTs' solubility, whereas a lower amount of impurities may be achieved resulting into a lower toxicity.

The structural and textural characteristics of the modified materials have been studied using different techniques. The main structural changes observed from IR spectra and thermal analyses are an increase of the carboxyl groups and an increase of the oxidation temperature as the treatment time increases. Raman spectroscopy has allowed us to estimate the disorder of the nanotubes. We have concluded that for short times the disorder decreases, whereas for long oxidation time it increases.

Regarding the textural properties, the N_2 adsorption-desorption isotherms of the modified nanotubes have allowed us to determine the specific surface area, which increases with the oxidation time, and the pore size distribution.

Keywords: MWCNT, functionalized nanotubes, acid treatment, mild oxidation

Table of Contents

Resumen	ii
Abstract	ii
Table of Contents	iii
List of Figures	iv
Acknowledgments	v
1 Introduction	1
2 Experimental techniques	3
2.1 Oxidation	3
2.2 Thermogravimetric analysis, Differential Scanning Calorimetry and Mass Spectroscopy (TG-DSC-MS)	3
2.3 Fourier Transform Infrared Spectroscopy (FTIR)	3
2.4 Raman Spectroscopy	3
2.5 Adsorption - Desorption of nitrogen isotherms	4
2.6 Transmission Electron Microscopy (TEM)	4
3 Results and discussion	5
3.1 Thermogravimetric analysis, Differential Scanning Calorimetry and Mass Spectroscopy (TG-DSC-MS)	5
3.2 Fourier Transform Infrared Spectroscopy (FTIR)	7
3.3 Raman Spectroscopy	9
3.4 Adsorption - Desorption of nitrogen isotherms	12
3.5 Transmission Electron Microscopy (TEM)	17
4 Conclusions	19
Bibliography	20
Appendices	
Appendix 1: Biological experiments	23
Appendix 2: Errors	25

List of Figures

1.1	Characteristics and structures of MWCNT, SWCNT and graphene.	1
3.1	TG (left) and DTG (right) measurements for all the samples.	5
3.2	Weight residue and oxidation temperature versus oxidation time.	6
3.3	DSC and MS-CO ₂ signal.	7
3.4	FTIR spectrum for the pristine nanotube.	8
3.5	FTIR spectra for all samples.	9
3.6	Raman spectrum for the pristine nanotube.	10
3.7	Disorder measure by two different methods using Raman measurements.	11
3.8	Peaks center's displacement measured via Raman spectroscopy.	12
3.9	Adsorption-desorption isotherm of nitrogen for the pristine sample.	13
3.10	Nitrogen isotherms for pristine, 4h and 24h samples.	14
3.11	Pore size distribution for the pristine sample (BJH method).	15
3.12	Pore size distribution for pristine, 4h and 24h samples (BJH method).	15
3.13	BET specific surface area (SSA) and pore diameter obtained by BJH method.	16
3.14	TEM diameter measure of MWCNTs versus oxidation time.	17
3.15	TEM image of the pristine sample.	18
A.1	Photograph showing dead and alive cells.	23
A.2	Survival rate of cells versus time.	24

Acknowledgments

This work has been done thanks to the financial project from the MINECO-ISCI Ref. PI13/01074 AES 2013. Apart from that, Jesus González has collaborated with the Raman spectroscopy, and Lidia Rodriguez with the TEM images.

Also, I would like to thank my supervisor at the University of Cantabria, Carmen Pesquera, and the department of “Química e Ingeniería de Procesos y Recursos” at the University of Cantabria for allowing me to work with them and for being very patient and helpful.

Lastly, thanks to my little brother for always being there.

1. Introduction

Carbon is known for being one of the elements with the richest family of allotropes, ranging from the well known diamond and graphite, to the newer nanotubes.

Carbon nanotubes were first discovered on their multi-walled version (MWCNT) by Ijima in 1991 [1], whereas the single-walled nanotubes (SWCNT) were reported by two teams almost simultaneously two years later [2, 3].

Graphene is a two-dimensional structure made of planar sp^2 bound carbons with a thickness of only one atom. MWCNT are made of concentric graphene sheets rolled up creating cylinders with diameters within the nanometers scale. Capping some of these cylinders there is half of a fullerene-like molecule consisting in five or seven membered ring.

Typically, MWCNTs can have from 2 to 50 layers, with a separation between them of *ca* 0.34 nm [4]. When they are synthesized by Chemical Vapor Deposition (CVD) methods, metal catalysts are usually used. Starting from the metal surface, the nanotube starts growing upwards until it gets capped by an impurity such as amorphous carbon, an aromatic carbon or a polyhedral carbon [5].

Because of the covalent bonds between carbon atoms in rings, MWCNTs are extremely hydrophobic. This causes them to aggregate and form bundles due to van der Waals interactions between their walls.

To state some differences and in order to see how diverse carbon structures can be in MWCNT, SWCNT as well as graphene, we have included the Figure 1.1, which represents a brief summary of their main characteristics.

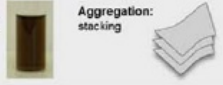
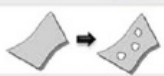
Physicochemical Characteristics	Graphene	Carbon Nanotubes	Difference
Shape	Planar – monolayer or multi-layer ; tunable structure/shape (sheet, ribbon, triangle, hexagon) 	Cylindrical Single-walled SWCNT Multi-walled MWCNT 	Completely different
Dimensions (typical)	Thickness: 0.34 -100nm Lateral size 0.3 -10µm 	SWCNT: L: 10nm to 1cm D: 0.4 - 3 nm MWCNT: L: 10nm to few microns D: 2–200 nm	Similar
Surface • Area • Charge • Coating	<ul style="list-style-type: none"> Up to 2675m²/g; decrease with layer number varies with functionalization or coating varies with chemical nature (polymer, lipid), type, density & conformation 	<ul style="list-style-type: none"> SWCNT (>1000 m²/g) ; MWCNT (100-500m²/g) varies with functionalization or coating varies with chemical nature (polymer, lipid), type, density & conformation 	<ul style="list-style-type: none"> • Quite different • Similar • Similar
Elasticity/Stiffness	Young modulus of 1100 GPa; able of bending and ripping; stiffness increases with number of layers	SWCNT from 1 to 5 TPa; able of bending MWCNT from 0.2 to 0.95 TPa	Similar
Colloidal stability • Aqueous dispersibility • Aggregation	Dispersibility: Graphene oxide in water Aggregation: stacking 	Dispersibility: Oxidized CNT in water Aggregation: bundling and tangling 	Very different
Durability	 Enzymatic degradation by defects in plan	 Enzymatic degradation by unzipping and decrease of L & D	Different
Impurities	Varies with manufacturing process; mainly graphite and chemical residues from processing	Varies with manufacturing process; metal catalysts (Fe, Co, Ni, Cr, Cu, Zn) ; carbon nanoparticles ; amorphous carbon	Very different

Figure 1.1: Characteristics and structures of MWCNT, SWCNT and graphene. Image taken from [6]

1. Introduction

As previously mentioned, pristine MWCNT are electrostatically charged and hydrophobic. In order to make them more soluble, we have to increase their hydrophilic behavior and reduce its toxicity by oxidizing the nanotubes using acid treatments as a previous step for further functionalization. Functionalization is a chemical process that inserts functional groups, which can facilitate the incorporation of other molecules that may be useful for many different applications. Oxidation can take place as either:

- Gas phase treatment: Employs a gaseous agent which will increase the hydroxyl and carbonyl groups concentrations. It is also capable of removing amorphous carbon/carbonaceous impurities.
- Liquid phase treatment: When the agent is in liquid form it is usually able to raise the concentration of carboxylic acid groups [7]. It can also decap and shorten MWCNTs, along with eliminating metal catalysts and another carbon allotropes. As a downside, with a strong oxidizing acid or long times [8], the structure of the nanotubes can be damaged, reducing their mechanical and electronic properties.

Therefore, it is important to establish a well-defined relationship between the functionalization parameters (acid concentration, treatment time) and the damage a nanotube can support without deteriorating its properties.

The hydrophilic nature of these functional groups that have been inserted led to a reduction of the Van der Waals interactions, which improves MWCNTs' solubility, whereas a decrease on the quantity of impurities may result into a lower toxicity. Then, using a liquid phase treatment we should have been able to achieve the two factors mentioned above, which is why the approach we have taken in the present work includes the usage of liquid acids.

One of the potential applications of MWCNTs is cancer treatment, which requires a decrease on the nanotubes' toxicity. This is possible due to the similarity in scale, as they both self-assemble and form bundles, between nanotubes and microtubules, which are the structures in charge for the division and movement of the cell on eukaryotic cells. The nanotubes are able to enter easily on the cell due to its sharp aspect ratio, and once inside they can form a biosynthetic polymer mixing with the microtubules, which causes the apoptosis of the cell.

Hence, the main concerns that need to be addressed in order to progress with the biological applications of the nanotubes are:

- Specificity: As we want them to attack only the selected cells
- Toxicity: As we need to deliver them only to the tumorous zone,
- Biodegradability: Because we would like to be able to get rid of them after their task is completed, in order to avoid side effects due to their presence as a foreign body.

In this work we have attempted to improve MWCNTs properties regarding the two last points mentioned above. In order to do so, we have employed a set of techniques described on the following section, which are able to provide us with an insight of the changes produced by the oxidation process we have carried on. Therefore, the goal of this work is to characterize a commercial sample of MWCNTs using a variety of physicochemical techniques, and modify and study the modifications induced by acid treatments.

2. Experimental techniques

Here we have described briefly the experimental techniques used in the present work. First, we have described how the sample oxidation was done, and then we have commented the experimental techniques employed for the characterization.

2.1 Oxidation

A mixture of $\text{HNO}_3/\text{H}_2\text{SO}_4$ (1:3 v/v) 6M with *ca* 0.3 g of the commercial sample (>95% purity) MWCNTs Nanocyl 3100 prepared by Catalytic CVD [9] was used. These nanotubes' average diameter as advertised by the manufacturer is 9.5 nm and its average length is 1.5 μm . The procedure was as follows:

1. MWCNTs were dispersed by sonication in a conventional ultrasonic bath for 15 minutes with Ultrasons, Selecta, with a power of 110 W and a frequency of 50 kHz.
2. Then, the mixture was kept at reflux for different times (4, 12 and 24 hours) with a heating plate at 150°C and magnetically stirring the mélange at 125 RPM.
3. Next, the samples were washed and filtered with deionized water on a Buchner funnel with a filter paper of *ca* 0.45 μm pore diameter until pH neutrality was obtained.
4. Finally, samples were collected and dried it in vacuum for 24 hours at 100°C.

2.2 Thermogravimetric analysis, Differential Scanning Calorimetry and Mass Spectroscopy (TG-DSC-MS)

The thermogravimetric analysis were carried out by a Setaram Setsys Evolution apparatus, ranging from *ca* 20 - 1000 °C. Measurements were performed in air as well as nitrogen atmosphere with a heating rate of 10 °C/min. A mass spectrometer, Pfeiffer OmniStar Prisma, attached to the TG allowed us to follow the gases (H_2O and CO_2) produced during the combustion process.

2.3 Fourier Transform Infrared Spectroscopy (FTIR)

Using a Jasco LE4200 spectrophotometer, measurements were performed by doing 264 scans between 400-4000 cm^{-1} with a resolution of $\pm 2 \text{ cm}^{-1}$ on pellets made of KBr:Sample on a weight proportion 300:1. Then, spectra was corrected by subtracting a baseline and eliminating the H_2O and CO_2 signal, and smoothed by the "Adjacent Averaging Method" of 25 points.

2.4 Raman Spectroscopy

Raman spectra were obtained from a Horiba T64000, property of the Departamento de Ciencias de la Tierra y Física de la Materia Condensada (CITIMAC). The samples were deposited on glass slides, and excited through a 20X microscope objective with an Ar laser beam of 514 nm

and a power of 20 mW over the sample. Scans were taken in the 1200 - 3300 cm^{-1} range for the general spectra, and in the range 95 - 750 cm^{-1} to get information about the Radial Breathing Mode (RMB) of the nanotubes.

2.5 Adsorption - Desorption of nitrogen isotherms

Adsorption - Desorption cycles were measured by low-temperature nitrogen technique using Micromeritics ASAP-2010 apparatus. Before the analysis, the samples were degassed at 140°C for 8 hours before test. Then, different formalisms were used on the raw data, such as Brunauer, Emmet and Teller (BET [10]) to determine the specific surface area and Barrett, Joyner and Halenda (BJH [11]) to obtain the pore size distribution at the mesoporous region.

2.6 Transmission Electron Microscopy (TEM)

The images presented at this work were obtained by the Servicio de Microscopia Electrónica de Transmisión (SERMET) at the University of Cantabria, using a JeoL JEM 2100 with a LaB₆ filament at 120 kV.

The nanotubes were sonicated for five minutes using Elma Sonic SH-15, and then dispersed on MeOH. Then, one droplet was dropped on a copper grid coated with C holey from Agar Scientific.

3. Results and discussion

On the following, we will refer to the different samples as p, for the pristine (commercial, untreated [9]) nanotubes, p-Ox as the commercial oxidized sample (Series 3101), and Ox4h, Ox12h y Ox24h, or simply 4h, 12h and 24h for the MWCNTs which were treated that amount of time with the oxidizing agents. To include the p-Ox sample in the comparative graphs, we have assigned an arbitrary value of 1 hour for it, although it should always be clear that the treated samples were all made from the pristine sample, and that the commercial oxidized sample is just included for the sake of comparison.

3.1 Thermogravimetric analysis, Differential Scanning Calorimetry and Mass Spectroscopy (TG-DSC-MS)

We have represented in Figure 3.1 the TG measurement, which plots the weight measured as a function of the temperature for all the different samples under air atmosphere. It seems like the most oxidized samples resembles a closer behavior to the pristine nanotube, whereas the less oxidized (4h) is closer to the commercial oxidized, which we believe has had the weakest oxidation treatment.

Also, we have presented at Figure 3.1 the derivative of the TG signal. As we can see, there is one intense peak that can be used to identify the oxidation temperature of the samples and the weight loss corresponding to the formation of CO₂ and H₂O in the heating process with the oxygen of the air atmosphere much more clearly, as well as the initiation and final temperature of the process. Also, in p-Ox and 12h samples there is a very small peak assigned to the water loss at temperatures lower than 75°C, and maybe it can only be seen in these samples due to storage conditions or environmental fluctuations (e.g, humidity).

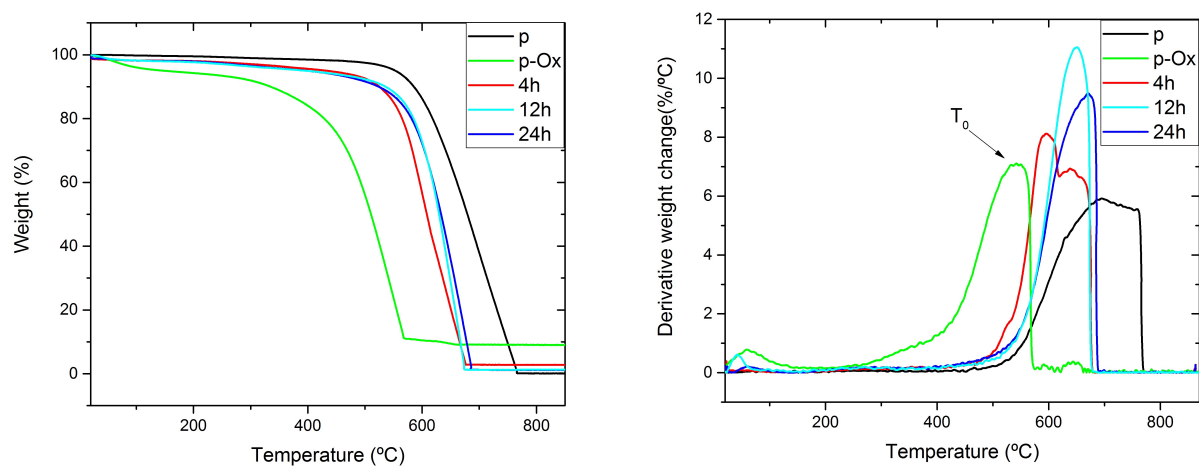


Figure 3.1: TG (left) and DTG (right) measurements for all the samples.

The oxidation temperature (T_0) and weight residue (intercept with the right axis in TG) determined by Figure 3.1 has been plotted on the Figure 3.2. On it, we can appreciate that the weight residue increases up to 4 hours of treatment, and then decreases quite slowly. However, the oxidation temperature follows an opposite trend, as it decreases very steeply, and then increases at a moderate rate. It is worth remembering at this point that a oxidation time of 1 hour represents the point of the commercial oxidized sample, which we have not treated in any way. It can be seen that, without taking into consideration this sample, both parameters have a less abrupt change.

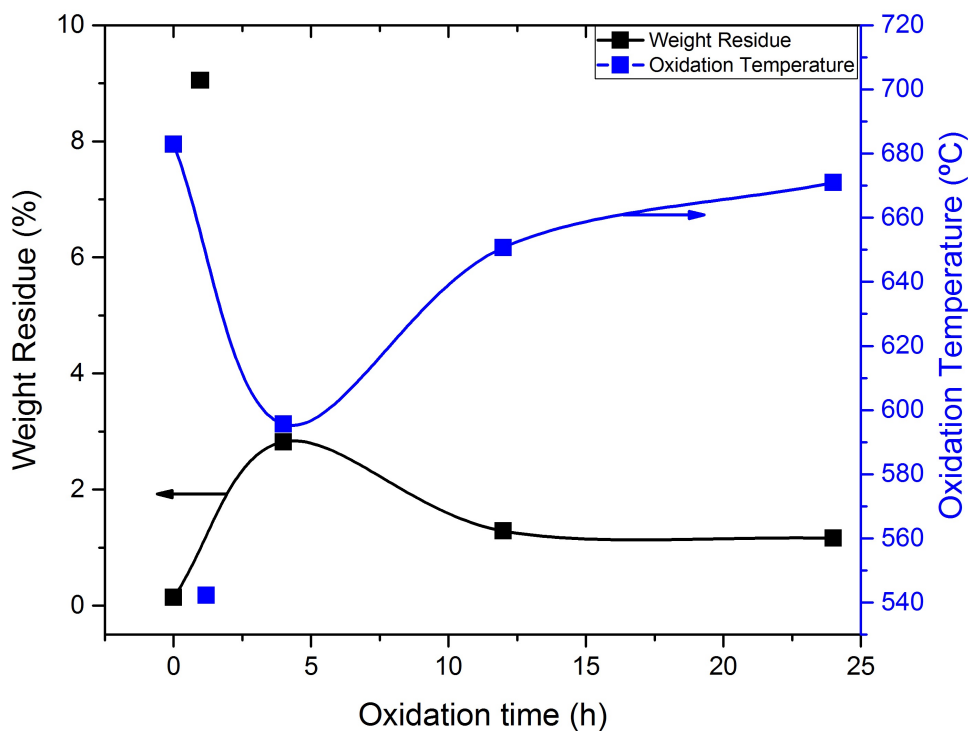


Figure 3.2: Weight residue as black filled squares at the left axis, oxidation temperature as blue filled squares at the right axis. The line between them is an spline, not a fit, for visual clarification.

Finally, by using the Mass Spectrometer, we have been able to represent the DSC with the MS signal together. From Figure 3.3, we have checked that most of the heat during the combustion reaction is due to the production of CO_2 , as both peaks are almost overlapping at the same temperature range with a small but visible offset caused by a slightly higher travel-time for the gases to reach the mass spectrometer.

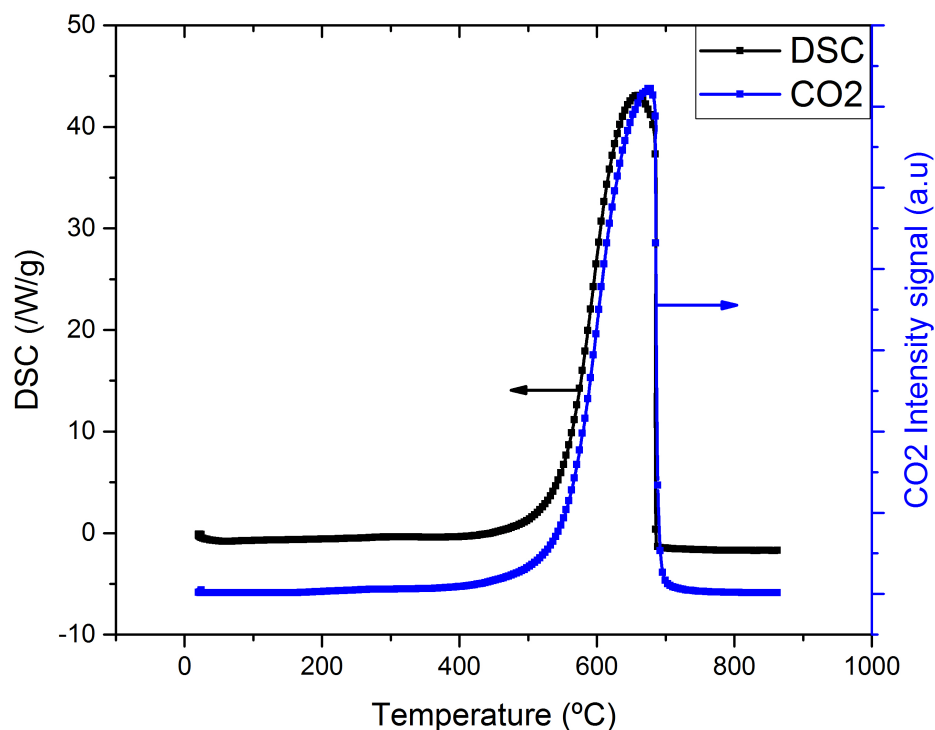


Figure 3.3: DSC (left axis) and CO₂ signal (right axis) obtained by the MS versus temperature for the sample Ox24h.

Therefore, with the the data presented in this section we have concluded that the thermal stability of the nanotubes remains unaltered, as the weight residue variation is less than 2.5% and the oxidation temperature absolute change is almost 80°C, but the decomposition temperature is still at a very high temperature, so future applications still have a broad range of temperature to work within.

3.2 Fourier Transform Infrared Spectroscopy (FTIR)

We have performed FTIR measurements as described in Section 2.3. First we have represented the spectrum for the pristine nanotubes and the peaks's position and label of the functional groups on Figure 3.4. All the spectra are shown together on Figure 3.5 for a better visual comparison between them. We have started identifying groups at *ca* 1500 cm⁻¹, using different bibliographic sources as [12–17]. It is worth notice that the pristine sample already has carbonyl and carboxylic groups, so it has already been oxidized partially.

As we can see, there are no big differences, and just small variations (extra differences are also on the lower wavenumber region, which we have not studied) on the peaks center

3.2. Fourier Transform Infrared Spectroscopy (FTIR)

and intensity of the different bands corresponding to different vibrations. Carboxylic group band at 1714 cm^{-1} has been seemed to increase as the oxidation time increases, whereas the aromatic C=C bond at 1563 cm^{-1} almost disappeared at 12 and 24 hours, showing a loss of aromaticity at graphitic walls. With a four hours treatment, the band increases, which may indicate a purification process. Carbonyl groups (C=O at 1650 cm^{-1}) have the same behavior as C=C.

An study regarding integral intensities on different bands, such as C=O / C=C has been carried out, although no conclusive results were obtained, so it has not been presented here.

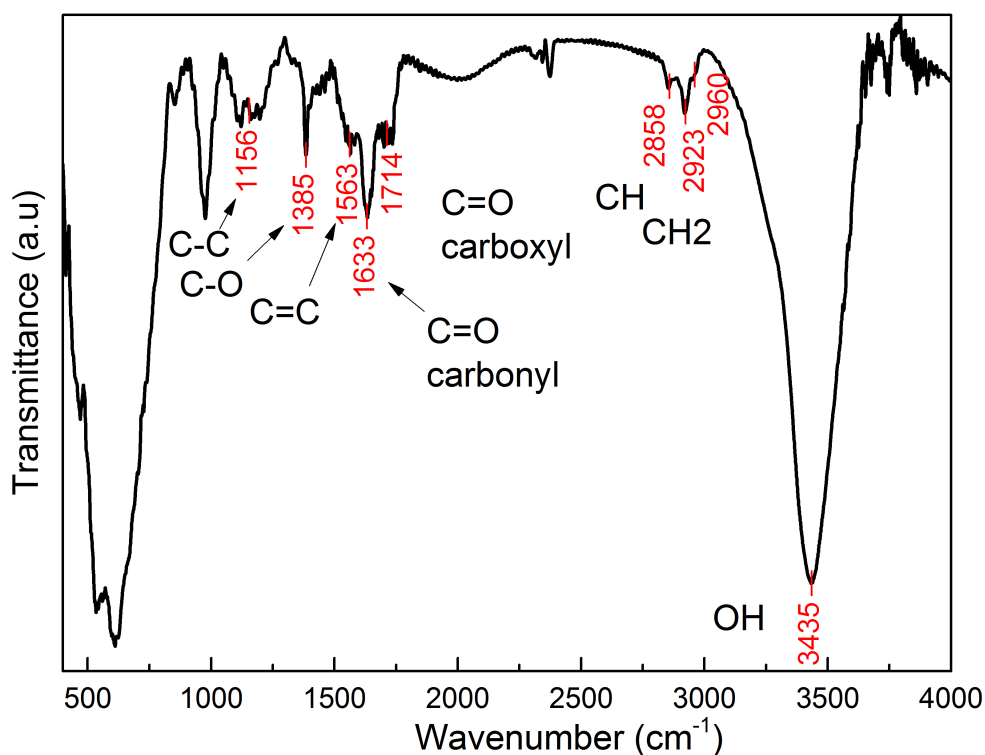


Figure 3.4: FTIR spectrum for the pristine nanotube, showing transmittance in arbitrary units versus wavenumber. Functional groups and its position has been marked.

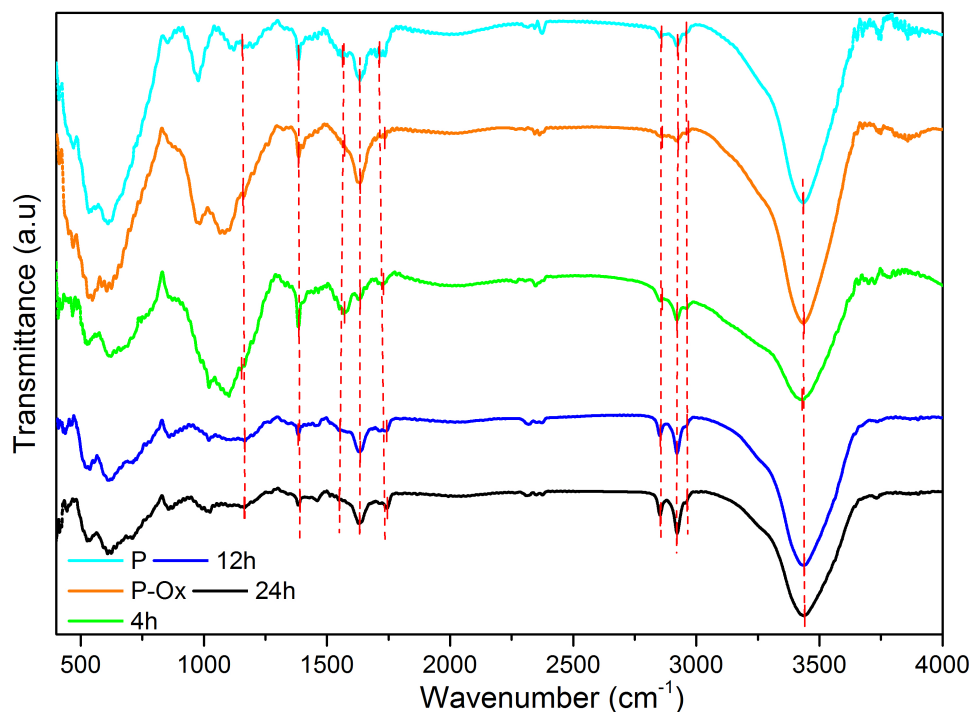


Figure 3.5: FTIR spectra for all the samples. Dashed red lines indicate the peaks's center shift.

3.3 Raman Spectroscopy

Raman spectra of carbon allotropes have been widely known and studied for a long time, as it can be used to identify different compounds and to provide a lot of useful information with a straightforward and quick scan. Here we have presented the Raman spectrum for the pristine nanotube in Figure 3.6, where all the characteristic peaks for carbon nanotubes have been identified. Its description has been omitted, as it can be found elsewhere [18].

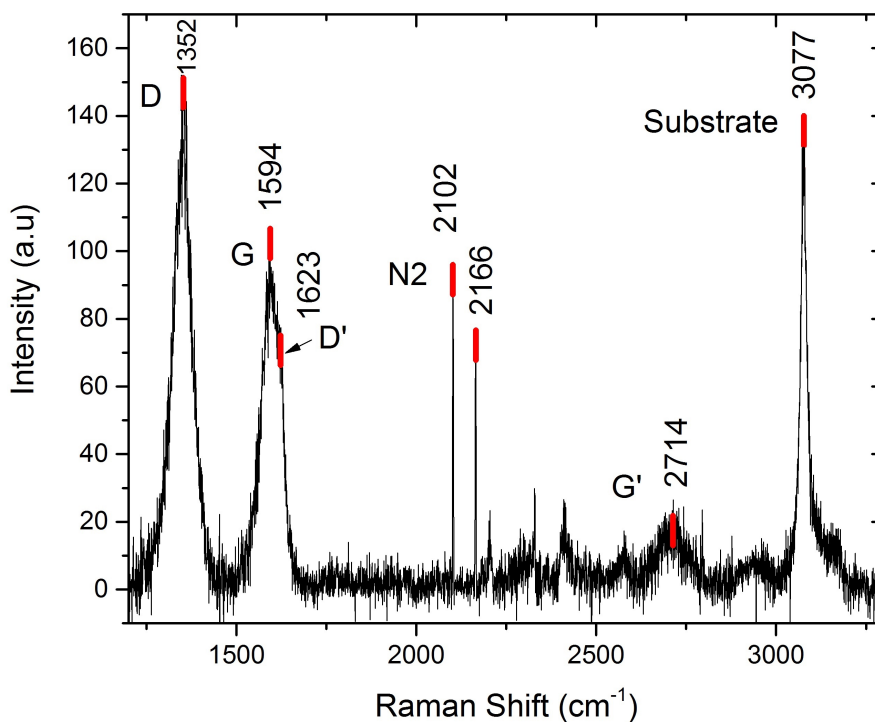


Figure 3.6: Raman spectrum for the pristine nanotube. Main peaks labeled (nitrogen peaks due to the atmosphere), identified and its centers indicated by a red line.

We have fitted the D, G and D' bands as pseudo-Voigt peaks with the gaussian full width half maximum (FWHM) fixed as the known instrumental broadening ($FWHM \approx 0.6 \text{ cm}^{-1}$). Then, we have determined the intensity ratio (as the maximum intensity of each peak) between the D and G band and the integrated area of those peaks to get a measurement of the disorder [19]. This was done in order to double-check that the same behavior was observed by both approaches, although we believe that the area ratio method should be more reliable, as it allows an error estimation due to propagation of the numerical error obtained through the fitting. A disorder estimation using these methods is possible due to the fact that the D (“Disorder”) band signal comes essentially from defects, so its signal increases as the concentration of defects increases, whereas the G band is supposed to be characteristic of the carbon nanotube.

From the Figure 3.7 we have observed that for small times (4h) the sample gets “ordered”, probably due to a reduction on metal catalyst impurities and amorphous carbon by the acids, and then the disorder increases monotonically. p-Ox sample at 1 hour is not connected by lines as the oxidation treatment performed on that sample is unknown.

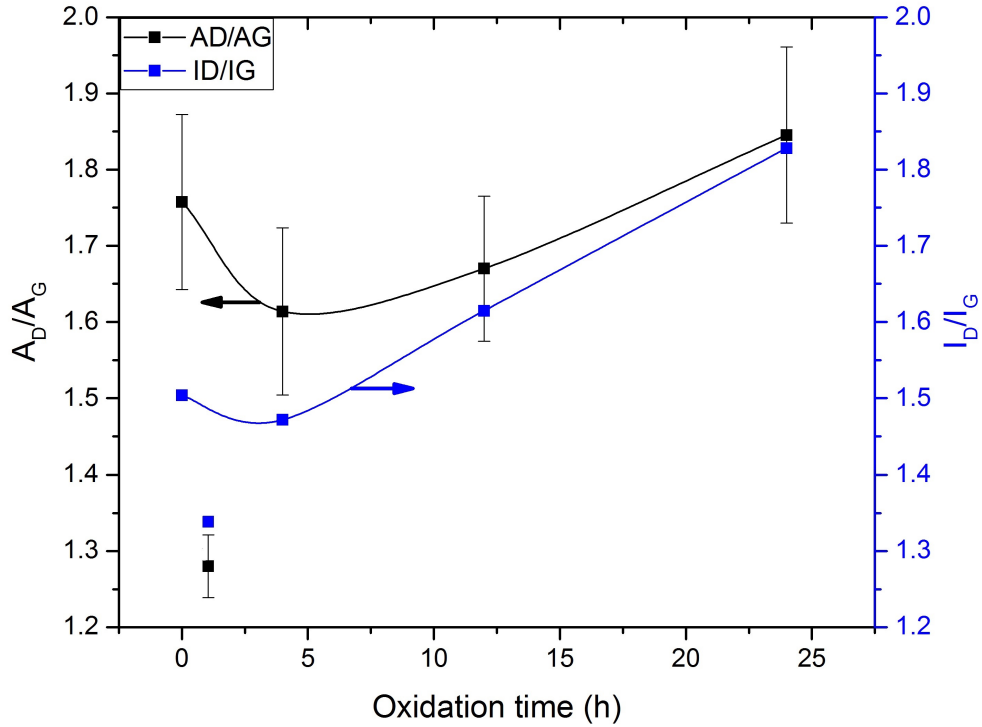


Figure 3.7: Area ratio (left) and intensity ratio (right) of D and G band as an indicator of the disorder. Lines are a spline connecting the points to serve as a visual guide.

Also, we have measured the Radial Breathing Mode (RBM) zone, between ca 150-300 cm^{-1} . RBM is useful to estimate the size of the nanotube. Using the empirical equation 3.1 from [18] and with the experimental peak center value obtained $\omega_{RMB} = 258 \pm 1 \text{ cm}^{-1}$, we have determined a diameter of $d \approx 0.9 \text{ nm}$, which would correspond to one of the innermost nanotubes,

$$\omega_{RMB}(\text{cm}^{-1}) = \frac{A}{d(\text{nm})} + \sqrt{1 + B \cdot d(\text{nm})^2} \implies d(\text{nm}) \approx \frac{234.14}{\omega_{RMB}(\text{cm}^{-1})} \quad (3.1)$$

where A is a constant which value is $A = 227.0 \pm 0.03 \text{ nm} \cdot \text{cm}^{-1}$, B is an environmental constant which ranges from 0.05 to 0.07 [20] and d is the diameter in nanometers.

RBM peak center value has been only possible to obtain at the pristine sample, while the others did not present a clear peak due to the extremely low signal produced in MWCNTs.

In Figure 3.8 we have represented the peaks's position with different oxidation time for the three bands, D, G and D'.

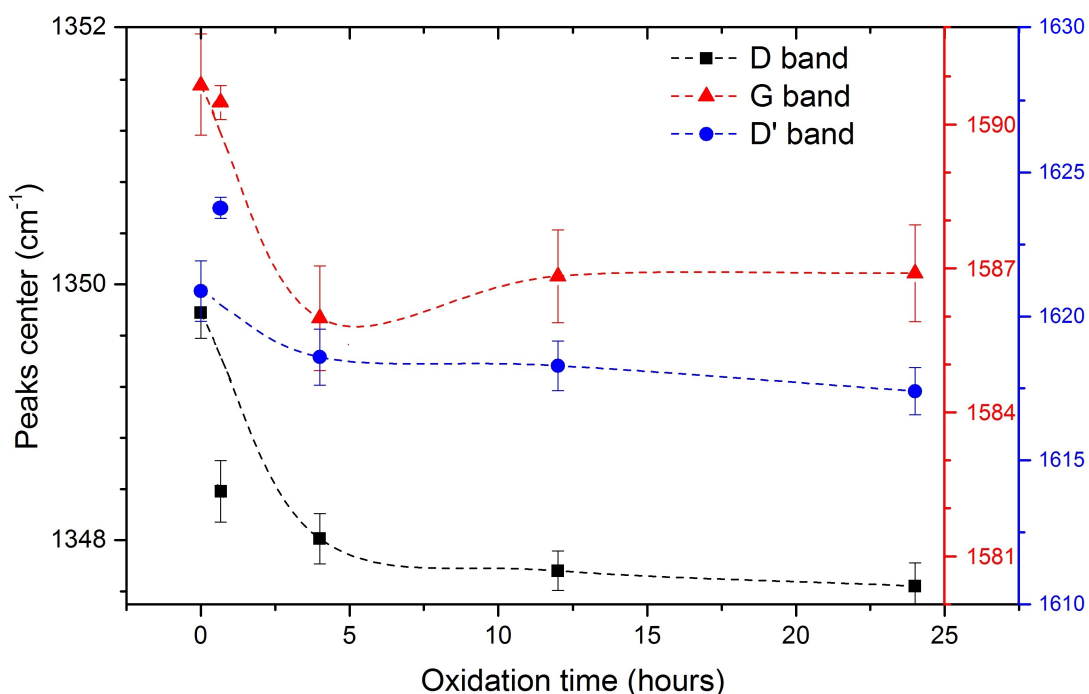


Figure 3.8: Peaks center for the D band (black squares), G band (red triangles) and D' band (blue circles) at different oxidation times. Lines are a spline to distinguish the trend.

When oxidation takes place, an addition of oxygen atoms may permit charge transfer to take place. The type of carrier (electron or holes) could be distinguished by either a red or a blue shift on Figure 3.8, respectively. In this case, as it goes to lower energy (lower wavenumber) it means that electrons are the charge carriers [21], although weakly, as the shift from pristine to 4 hour oxidation is around 5 cm^{-1} ($\approx 0.6 \text{ meV}$) for G band, and 2 cm^{-1} ($\approx 0.25 \text{ meV}$) for D and D' bands.

3.4 Adsorption - Desorption of nitrogen isotherms

Adsorption-desorption measurements have been performed as described previously, and BET [10] and BJH [11] formalisms have been applied to obtain the specific surface area and the pore diameter.

In Figure 3.9 we have represented the isotherm curve for the pristine sample including adsorption and desorption branch (upper part) showing the hysteresis loop formed between them, which indicates that both ends of the carbon nanotubes are open, as stated in [22].

At very low pressures, the isotherm is of Type I, with a very fast filling of pores within the molecular size, which indicates that there are micropores. The linear part, between 0.05 - 0.7 represents a surface adsorption process as a monolayer. The very high pressure zone, where the hysteresis loop is visible, corresponds to a capillary condensation process in mesopores, characteristic of Type IV isotherms. This adsorption has been attributed to aggregated pores

3.4. Adsorption - Desorption of nitrogen isotherms

formed in the structure made by the isolated nanotubes. These pores are believed to be the main source of capillary condensation, rather than the inner cavities of nanotubes [23].

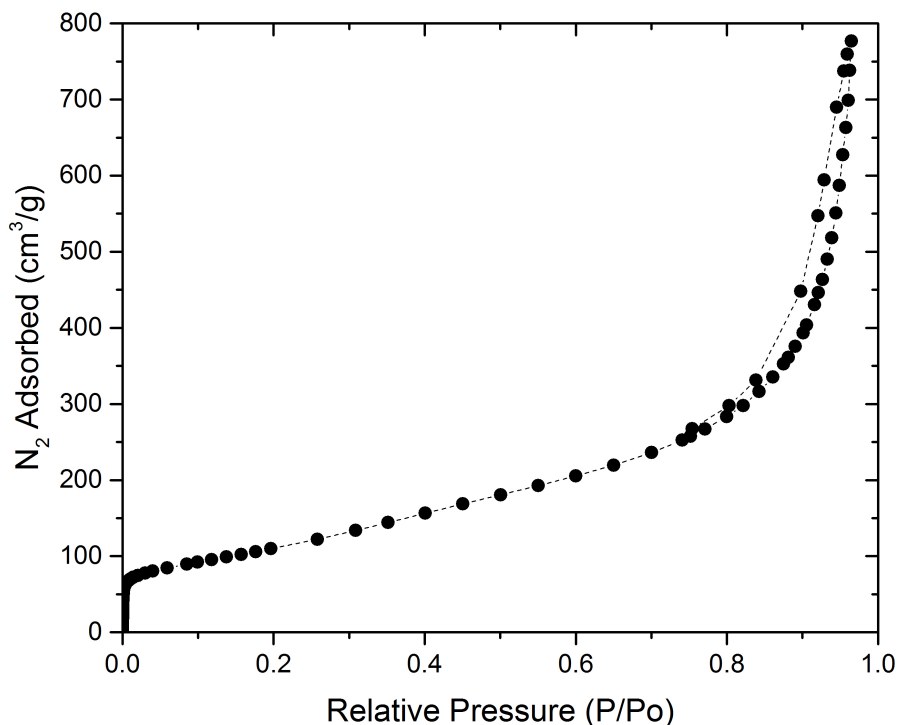


Figure 3.9: Adsorption-desorption isotherm of nitrogen against the relative pressure attained at the pristine sample.

The isotherms of the pristine, the minimum time and maximum time of oxidation have been included in Figure 3.10. As can be seen, there is no clear differences between, as all of them follow the trends specify in the previous paragraph, with a Type I behavior at low pressures, and Type IV at high pressures.

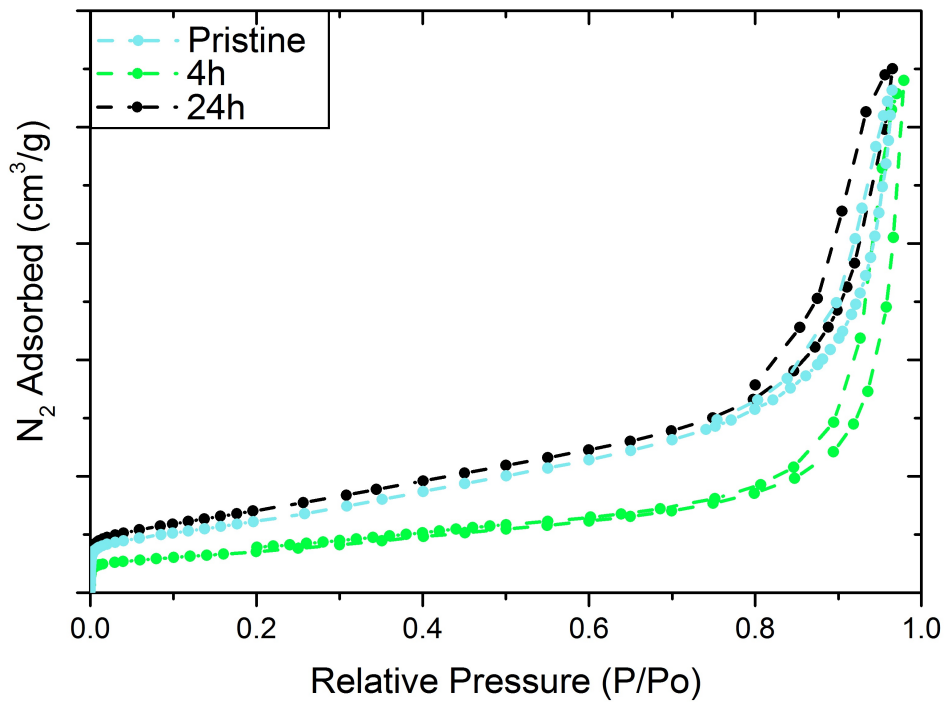


Figure 3.10: Nitrogen isotherms for pristine, 4h and 24h oxidized carbon nanotubes.

Also, we have included the BJH pore size distribution plot in the Figure 3.11 for the pristine sample, and a comparison between pristine, 4h and 24h oxidized sample at Figure 3.12. From it we can deduce that no big changes have been performed at the pore structure, as the pore size distribution curves are very similar one to another. Pore volume differences in this representation (Y axis) are, as mentioned when discussing the Figure 3.10, attributable to differences in the experimental method.

3.4. Adsorption - Desorption of nitrogen isotherms

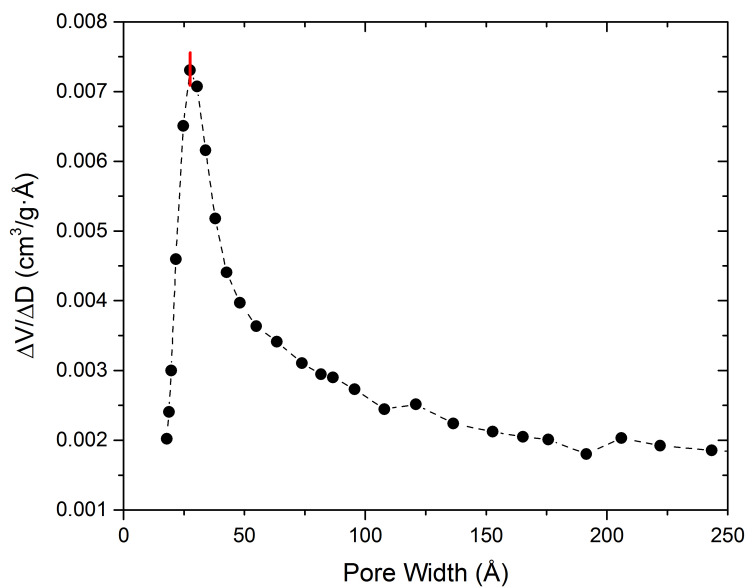


Figure 3.11: Pore size distribution for volume of nitrogen adsorbed for the pristine sample by BJH method. Peak center (taken as pore diameter) is indicated by a red line.

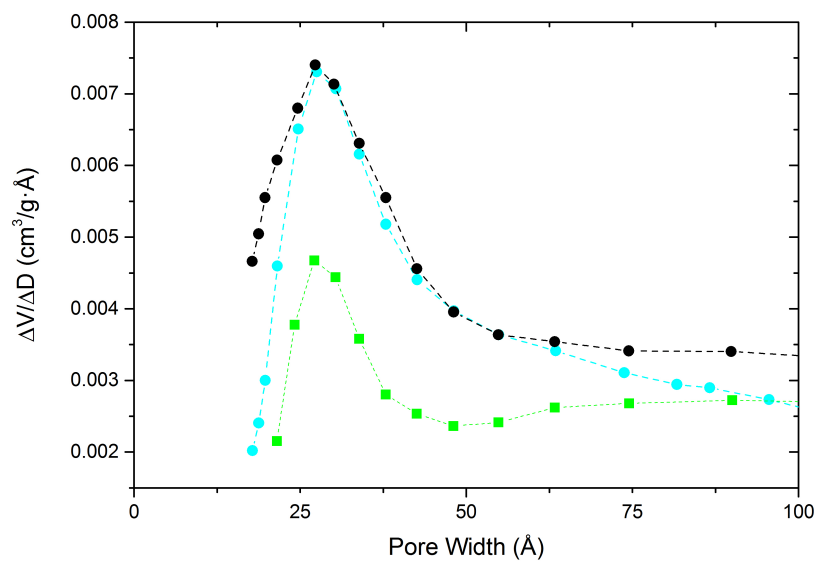


Figure 3.12: Pore distribution given BJH method for the pristine, 4h and 24h oxidized carbon nanotubes.

Using the previous figures and employing also the BET method, the aforementioned parameters (BET surface (surface specific area, SSA) and pore diameter) have been obtained and plotted against the oxidation time in Figure 3.13. From it, we have distinguished an increment on the surface by a factor of almost 20% for the sample oxidized 12 hours. For the pore diameters, we have seen that they remain almost unaltered (differences are less than 4%). Therefore, we have concluded that, although an increase in the surface area is achievable due to the fact that the structure of the nanotube is “opened” and the insertion of functional groups leads to an increase in the amount of binding spots, the main factor is the creation of inner cavities. Hence, the individual cylinder structure and the pores sizes remain unchanged.

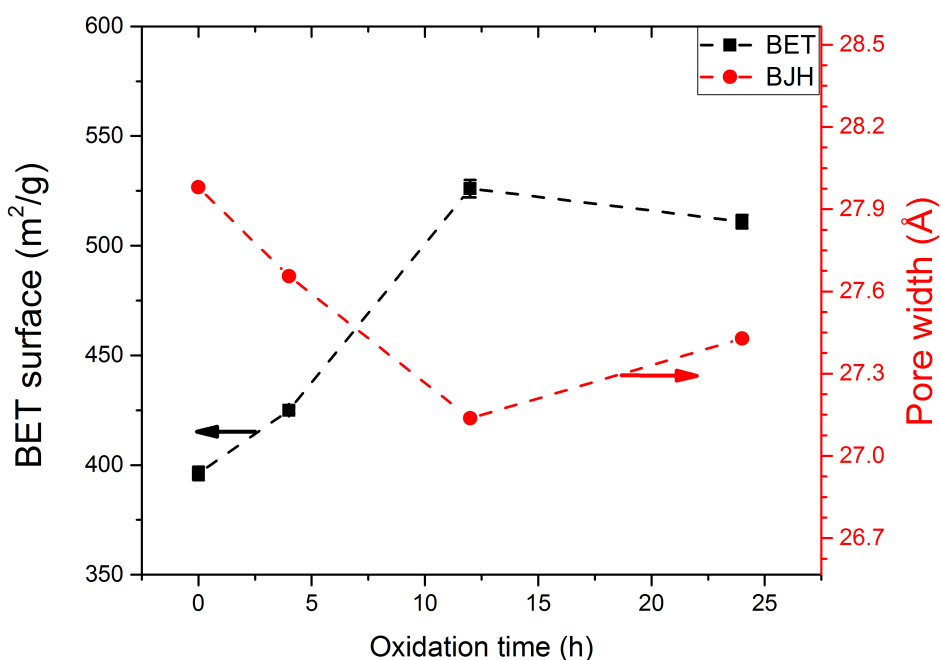


Figure 3.13: Parameters obtained (BET surface (black) and the pore width provided by BJH (red) method) versus the oxidation time.

Finally, I would like to mention, as future work, that some authors [22, 24] cite the method of using α -plots to obtain the micropores volume. This method, briefly, consists on sintering the material until it is not porous anymore and measure its isotherm. Then, we should represent the ratio of volume of nitrogen adsorbed by the sample to the quantity adsorbed by the sintered sample.

3.5 Transmission Electron Microscopy (TEM)

We have measured the inner, outer and the total diameter of the carbon nanotube for all the samples, and have represented it on Figure 3.14. The procedure was the following:

- On each photograph, we have measured each diameter ten times, in order to obtain the mean and standard deviation values.
- For each sample, we have repeated the previous step between 5 and 8 times on different nanotubes within the sample oxidation time, depending on the quality of the images.
- Then, the value was the average value between different photos for each samples, and the mean error (standard deviation over square root of the number of images) was propagated as relative error.

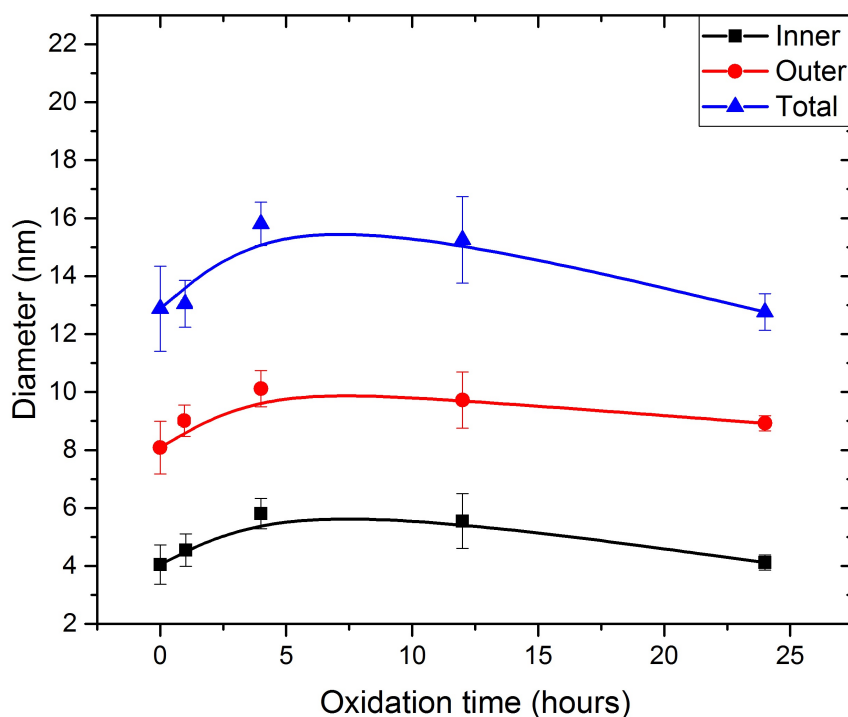


Figure 3.14: Diameter versus the acid treatment time. Line has been included as a visual guide.

Although a tendency is not clear due to relatively high errors and a small number of images analyzed, it appears that it follows the inverse trend as the disorder measurement performed by Raman spectroscopy (see Figure 3.7). This is, a small increase for the four hours treated

3.5. Transmission Electron Microscopy (TEM)

sample, and then a monotonically decrease. More measurements and statistical analysis should be performed in order to confirm this. With this measurement we have also confirmed that the outer diameter is in agree with the diameter value given by the manufacturer (9.5 nm).

At Figure 3.15 we have add some references as green lines in order to clarify which diameters have we referenced on the last discussion, and to show the structure of our nanotubes graphically.

The total diameter represents the whole structure, which includes the MWCNT plus the amorphous carbon layer adhered to its surface. The amorphous structure can be deduced from the fact that there is no ordered parallel lines (they indicate Miller planes), on contrary of what happen in the nanotube structure, where ordered lattice planes can be seen, a characteristic of crystalline structures.

The outer diameter corresponds to the outermost nanotube, inside of which there is more concentric carbon nanotubes one inside another.

Finally, the inner nanotube is the one with the smaller diameter. From the Figure 3.14 we have seen that the value is *ca* 4 nm, which is non compatible with the value obtained due to Raman spectroscopy of the RMB zone, which gave us a value around *ca* 1 nm. In any case, as mentioned in the Raman section, RMB spectra for this kind of MWCNT is not very clear and cannot be used as a method to obtain precise measurements, although both values are in the same order of magnitude.

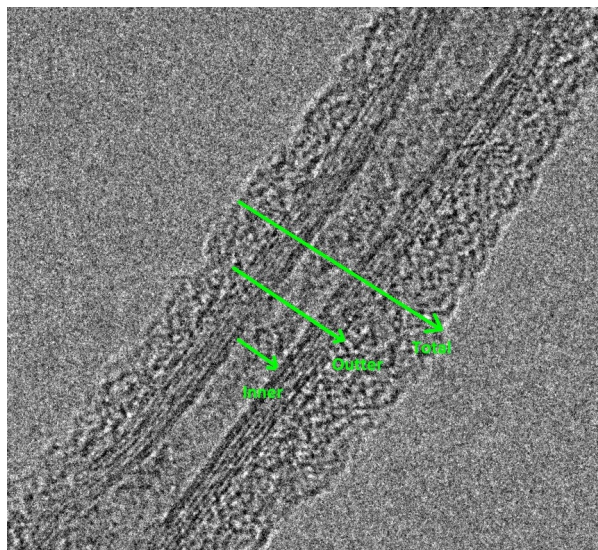


Figure 3.15: TEM image of the pristine sample, with straight green lines to exemplarize different diameters measured.

4. Conclusions

We have characterized five different multi-walled carbon nanotubes, two of them were commercial samples (pristine, and p-Ox, pristine oxidized) and three were samples of the pristine sample oxidized for 4, 12 and 24 hours. The main conclusions we have draw from our measurements are:

- Thermal stability: By means of TG, DTG, DSC and MS measurements we have been able to state that no big changes in the thermal stability of our samples take place for the oxidation times used. Weight residue variation is less than 2.5% and the oxidation temperature absolute change is around 80°C.
- Functional groups: Due to FTIR spectroscopy, it can be said that all spectra were very similar. The pristine sample already presented carbonyl and carboxylic groups, being at least partially oxidized. However, carboxylic group band (1714 cm^{-1}) increased with oxidation time, whereas the aromatic C=C bond at 1563 cm^{-1} decreased, showing a loss of aromaticity at graphitic walls.
- Order/disorder measurement: Thanks to the Raman spectroscopy, it has been observed that for small times (4h) the sample gets “ordered”, probably due to a reduction on metal catalyst impurities and amorphous carbon by the acids, and then the disorder increases monotonically. Also, we have observed a very small charge displacement (red shift), observable due to the bands’ peaks displacement.
- Textural properties: Adsorption-desorption of nitrogen isotherms have been used to characterize two important properties, the BET specific surface area, and the pore size distribution. The first parameter increases greatly due to the creation of inner cavities between the nanotubes, creating “bags” of empty space that can be filled with nitrogen. The second parameter, the pore size distribution, remains unaltered, with changes of less than 4%.
- TEM images: Three different diameters have been measured with this technique. One of these, the outter diameter, is compatible with the diameter given by the manufacturer company. Also, bundles of nanotubes formed when they are oxidized have been distinguished in the images. Finally, a simple study of the variation of the diameters showed very small changes, with a tendency opposite to the extracted with Raman.

To summarize, in this work it has been observed that even the pristine commercial sample has been already oxidized. Also, it has been checked that a mild oxidation treatment for times up to 24 hours does not produce appreciable changes, neither structural nor behavioral. Therefore, the 4h sample should be most ordered one, with very similar properties to the other nanotubes, but with less time of oxidation. If there is no need of improving these characteristics, then the pristine sample has a similar behaviour, plus saving time and money on the acid treatment.

Bibliography

- [1] S. Iijima. Helical microtubules of graphitic carbon. *Nature*, **vol. 354**(6348): pp. 56–58, 1991.
- [2] S. Iijima and T. Ichihashi. Single-shell carbon nanotubes of 1-nm diameter. *Nature*, **vol. 363**: pp. 603–605, 1993.
- [3] D. Bethune, C. Klang, M. De Vries, G. Gorman, R. Savoy, J. Vazquez, and R. Beyers. Cobalt-catalysed growth of carbon nanotubes with single-atomic-layer walls. *Nature*, **vol. 363**: pp. 605–607, 1993.
- [4] M. Yudasaka, R. Kikuchi, T. Matsui, Y. Ohki, S. Yoshimura, and E. Ota. Specific conditions for Ni catalyzed carbon nanotube growth by chemical vapor deposition. *Applied Physics Letters*, **vol. 67**(17): pp. 2477–2479, 1995.
- [5] X. Ling, Y. Wei, L. Zou, and S. Xu. The effect of different order of purification treatments on the purity of multiwalled carbon nanotubes. *Applied Surface Science*, **vol. 276**: pp. 159–166, 2013.
- [6] C. Bussy, H. Ali-Boucetta, and K. Kostarelos. Safety considerations for graphene: lessons learnt from carbon nanotubes. *Accounts of Chemical Research*, **vol. 46**(3): pp. 692–701, 2012.
- [7] Y.-T. Kim and T. Mitani. Oxidation treatment of carbon nanotubes: An essential process in nanocomposite with RuO₂ for supercapacitor electrode materials. *Applied Physics Letters*, **vol. 89**(3): p. 3107, 2006.
- [8] Y.-C. Chiang, W.-H. Lin, and Y.-C. Chang. The influence of treatment duration on multi-walled carbon nanotubes functionalized by H₂SO₄/HNO₃ oxidation. *Applied Surface Science*, **vol. 257**(6): pp. 2401 – 2410, 2011.
- [9] N. SA. Nanocyltm NC3100 series - product datasheet thin multi-wall carbon nanotubes. File available at : <http://www.nanocyl.com/en/content/download/419/2542/file/DM-TS&D-02-TDS>. Consulted at 16/06/2015.
- [10] S. Brunauer, P. H. Emmett, and E. Teller. Adsorption of gases in multimolecular layers. *Journal of the American Chemical Society*, **vol. 60**(2): pp. 309–319, 1938.
- [11] E. P. Barrett, L. G. Joyner, and P. P. Halenda. The determination of pore volume and area distributions in porous substances. i. computations from nitrogen isotherms. *Journal of the American Chemical Society*, **vol. 73**(1): pp. 373–380, 1951.

- [12] F. Aviles, J. Cauich-Rodriguez, L. Moo-Tah, A. May-Pat, and R. Vargas-Coronado. Evaluation of mild acid oxidation treatments for MWCNT functionalization. *Carbon*, **vol. 47**(13): pp. 2970 – 2975, 2009.
- [13] H. Gong, S.-T. Kim, J. D. Lee, and S. Yim. Simple quantification of surface carboxylic acids on chemically oxidized multi-walled carbon nanotubes. *Applied Surface Science*, **vol. 266**: pp. 219 – 224, 2013.
- [14] X. Ling, Y. Wei, L. Zou, and S. Xu. The effect of different order of purification treatments on the purity of multiwalled carbon nanotubes. *Applied Surface Science*, **vol. 276**: pp. 159 – 166, 2013.
- [15] A. Osorio, I. Silveira, V. Bueno, and C. Bergmann. H₂SO₄/HNO₃/HCl functionalization and its effect on dispersion of carbon nanotubes in aqueous media. *Applied Surface Science*, **vol. 255**(5, Part 1): pp. 2485 – 2489, 2008.
- [16] K. Peng, L.-Q. Liu, H. Li, H. Meyer, and Z. Zhang. Room temperature functionalization of carbon nanotubes using an ozone/water vapor mixture. *Carbon*, **vol. 49**(1): pp. 70 – 76, 2011.
- [17] T. A. Saleh. The influence of treatment temperature on the acidity of MWCNT oxidized by HNO₃ or a mixture of HNO₃/H₂SO₄. *Applied Surface Science*, **vol. 257**(17): pp. 7746 – 7751, 2011.
- [18] M. S. Dresselhaus, A. Jorio, M. Hofmann, G. Dresselhaus, and R. Saito. Perspectives on carbon nanotubes and graphene Raman spectroscopy. *Nano Letters*, **vol. 10**(3): pp. 751–758, 2010.
- [19] M. S. Dresselhaus, A. Jorio, A. G. Souza Filho, and R. Saito. Defect characterization in graphene and carbon nanotubes using Raman spectroscopy. *Philosophical Transactions of the Royal Society of London A: Mathematical, Physical and Engineering Sciences*, **vol. 368**(1932): pp. 5355–5377, 2010.
- [20] P. T. Araujo, I. O. Maciel, P. B. C. Pesce, M. A. Pimenta, S. K. Doorn, H. Qian, A. Hartschuh, M. Steiner, L. Grigorian, K. Hata, and A. Jorio. Nature of the constant factor in the relation between radial breathing mode frequency and tube diameter for single-wall carbon nanotubes. *Physical Review B*, **vol. 77**: pp. 241403–1:241403–4, 2008.
- [21] C. Rao and R. Voggu. Charge-transfer with graphene and nanotubes. *Materials Today*, **vol. 13**(9): p. 34:40, 2010.
- [22] S. Inoue, N. Ichikuni, T. Suzuki, T. Uematsu, and K. Kaneko. Capillary condensation of N₂ on multiwall carbon nanotubes. *The Journal of Physical Chemistry B*, **vol. 102**(24): pp. 4689–4692, 1998.
- [23] Q.-H. Yang, P.-X. Hou, S. Bai, M.-Z. Wang, and H.-M. Cheng. Adsorption and capillarity of nitrogen in aggregated multi-walled carbon nanotubes. *Chemical Physics Letters*, **vol. 345**(1): pp. 18 – 24, 2001.

- [24] M. Eswaramoorthy, R. Sen, and C. Rao. A study of micropores in single-walled carbon nanotubes by the adsorption of gases and vapors. *Chemical Physics Letters*, **vol. 304**(3-4): pp. 207–210, 1999.

Appendix 1: Biological experiments

As mentioned in the Introduction, one of the important applications for acid-treated nanotubes would be a biological usage, so to achieve a reduction of the toxicity is an important task. Therefore, we have performed an easy experiment to show one of the possible ways to measure this toxicity and it is described on the following lines.

We have checked the survival rate of BV2 microglia cells (macrophages in the brain and spinal cord at murinae species). To do so, we have prepared a medium with Iscove's Modified Dulbecco's Medium (IMDM), serum and gentamicin (antibiotic), as well as phenol red to monitor the pH change (turns yellowish when the pH decreases) which is an indicator of the health of the cells.

Then, we have added the resuspended MWCNTs with a concentration *ca* 40 $\mu\text{g/ml}$. After that, at different times (24, 48 and 72 hours) we have lift off the cells from the bottom of the recipient and added 0.1 ml of trypan blue which is a dye that allows us to distinguish between dead and alive cells. Lastly, we have just counted the number of these cells on an optical microscope and have performed the statistic analysis.

As described before, we have been able to apply our nanotubes to macrophages, and see how different oxidation times affect its survival rate (alive/total cells). An example of how we have counted the cells on the microscope can be seen on the photograph included at Figure A.1

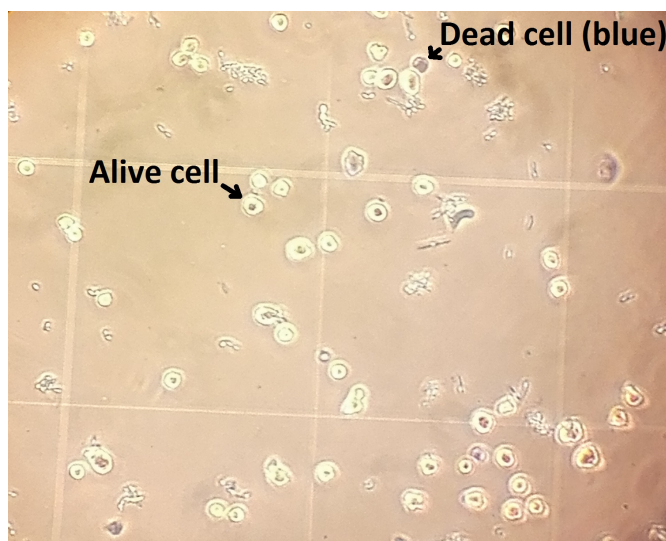


Figure A.1: Photograph of the counting process, distinguishing between dead (blue, darker) and alive cells

As shown on Figure A.2, where Control group means that no nanotubes were added, the lower survival takes place where the pristine nanotubes are added, but it increases with the oxidation time for 24h. Then, either at 48h and 72h, the values are very close to each other and

it is not possible to make any further appreciation apart from noticing that still the most oxidized nanotubes present the higher survivability.

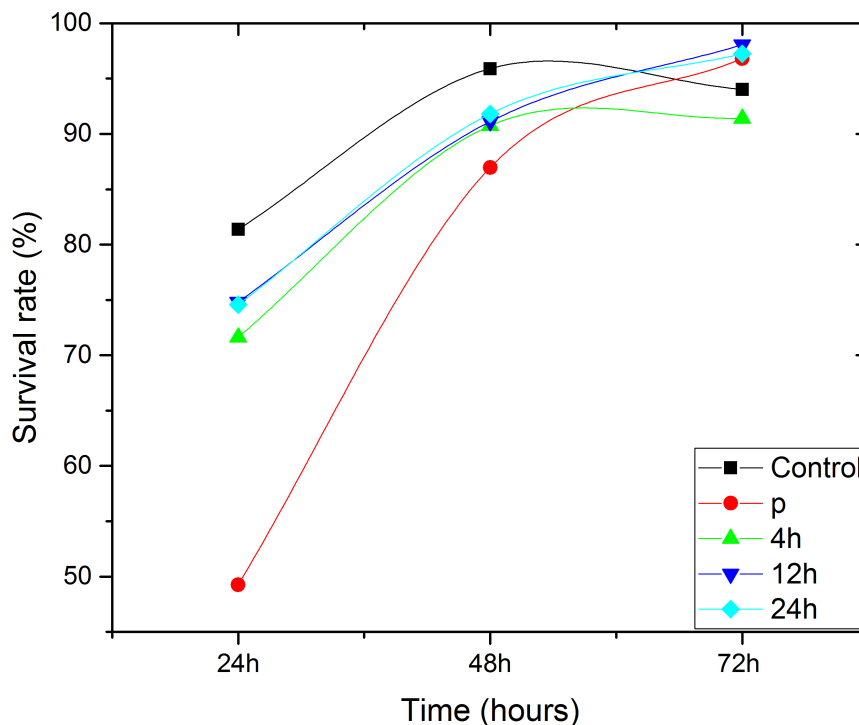


Figure A.2: Survival rate after 72 hours after applying different treated nanotubes. Lines provided as visual guides.

It is worth to mention that this experiment was not carried out as experts usually do, as a lot more of statistical measurements should have been performed in order to eliminate the individual fluctuations on such systems. Therefore, this section is just included to show how an experiment related have been carried out. In this case, a positive result has been obtained, although it should be confirmed by other techniques, as flow cytometry.

Appendix 2: Errors

The errors included in the Figure 3.7 have been calculated through the numerical errors given by the area determination by fitting the peak to a pseudoVoigt profile with fixed gaussian FWHM to account for the instrumental broadening. Hence, the error of the ratio was obtained with the following equation:

$$\delta \left(\frac{A_D}{A_G} \right) = \sqrt{\left(\frac{\delta A_D}{A_D} \right)^2 + \left(\frac{\delta A_G}{A_G} \right)^2} \left(\frac{A_D}{A_G} \right) \quad (1)$$

where A_D means the area of the D band, A_G of the G band, and δ the absolute error of the corresponding magnitude.

Regarding the errors shown in Figure 3.14, they were determined as follows:

- First, given an image, the different diameters were measured repeatedly for a certain nanotube, and mean and standard deviation was obtained.
- Then, the first step was repeated for a number of images at the same oxidation time, obtaining then the error corresponding to each different oxidation time sample as the standard error of the mean (standard deviation divided by the square root of the number of the sample size).